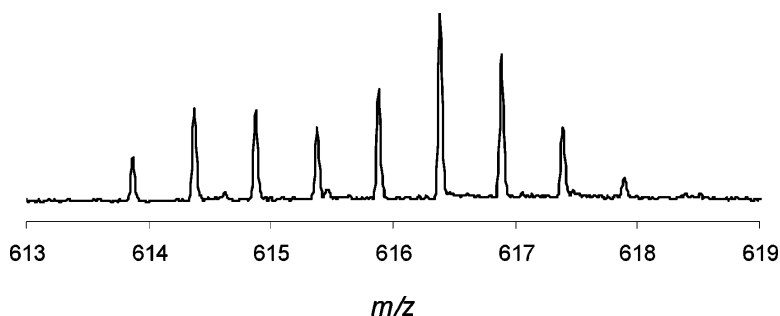


Intramolecular Migration of Amide Hydrogens in Protonated Peptides upon Collisional Activation

Thomas J. D. Jrgensen, Henrik Grdsvoll, Michael Ploug, and Peter Roepstorff

J. Am. Chem. Soc., **2005**, 127 (8), 2785-2793 • DOI: 10.1021/ja043789c • Publication Date (Web): 04 February 2005

Downloaded from <http://pubs.acs.org> on March 24, 2009



More About This Article

Additional resources and features associated with this article are available within the HTML version:

- Supporting Information
- Links to the 14 articles that cite this article, as of the time of this article download
- Access to high resolution figures
- Links to articles and content related to this article
- Copyright permission to reproduce figures and/or text from this article

[View the Full Text HTML](#)



Intramolecular Migration of Amide Hydrogens in Protonated Peptides upon Collisional Activation

Thomas J. D. Jørgensen,^{*,†,‡} Henrik Gårdsvoll,[‡] Michael Ploug,[‡] and Peter Roepstorff[†]

Contribution from the Department of Biochemistry and Molecular Biology, University of Southern Denmark, DK-5230 Odense M, Denmark, and Finsen Laboratory, Rigshospitalet, DK-2100 Copenhagen Ø, Denmark

Received October 12, 2004; E-mail: tjdj@bmb.sdu.dk

Abstract: Presently different opinions exist as to the degree of scrambling of amide hydrogens in gaseous protonated peptides and proteins upon collisional activation in tandem mass spectrometry experiments. This unsettled controversy is not trivial, since only a very low degree of scrambling is tolerable if collision-induced dissociation (CID) should provide reliable site-specific information from ¹H/²H exchange experiments. We have explored a series of unique, regioselectively deuterium-labeled peptides as model systems to probe for intramolecular amide hydrogen migration under low-energy collisional activation in an orthogonal quadrupole time-of-flight electrospray ionization (Q-TOF ESI) mass spectrometer. These peptides contain a C-terminal receptor-binding sequence and an N-terminal nonbinding region. When the peptides form a receptor complex, the amide hydrogens of the interacting sequences are protected against exchange with the solvent, while the amide hydrogens of the nonbinding sequences exchange rapidly with the solvent. We have utilized such long-lived complexes to generate peptides labeled with deuterium in either the binding or nonbinding region, and the expected regioselectivity of this labeling was confirmed after pepsin proteolysis. CID of such deuterated peptides, [M + 2H]²⁺, yielded fragment ions (b- and y-ions) having a deuterium content that resemble the theoretical values calculated for 100% scrambling. Thus, complete randomization of all hydrogen atoms attached to nitrogen and oxygen occurs in the gaseous peptide ion prior to its dissociation.

Introduction

Amide ¹H/²H exchange in combination with mass spectrometry has become a useful method to study the conformational properties of proteins and their complexes in solution.^{1–4} A unique advantage offered by this method is the ability to measure correlated exchange of amide hydrogens by the appearance of distinct bimodal isotopic envelopes in the mass spectra.⁵ This property has been exploited to study transient, cooperative unfolding events of proteins,^{6–9} protein folding intermediates,¹⁰

and dynamics of protein–peptides complexes.¹¹ Such structural transitions are not readily detectable by NMR spectroscopy.^{8,10} The use of amide hydrogen exchange combined with mass spectrometry to investigate protein structure was originally introduced by Zhang et al.¹² The traditional procedure for probing the native structure of proteins is to label the protein with deuterium by incubation in deuterated buffer at physiological pH. Isotopic exchange of the amide hydrogens in the main chain is subsequently quenched by acidification (pH 2.5) and cooling (0 °C). Under quench conditions the protein is fragmented by pepsin, and the resulting peptides are subsequently desalted in protiated solvents by reversed-phase chromatography. The resolution of the method is currently limited by the number and sizes of the peptides generated by proteolysis. In this particular setting, the broad specificity of pepsin is beneficial resulting in overlapping peptide sequences that can further increase the resolution of the deuterium assignments.¹² Gas-phase dissociation of deuterated peptides appears at first glance to offer an attractive alternative method to obtain single

[†] University of Southern Denmark.

[‡] Rigshospitalet.

- (1) Yan, X. G.; Watson, J.; Ho, P. S.; Deinzer, M. L. *Mol. Cell. Proteomics* **2004**, *3*, 10–23.
- (2) Konermann, L.; Simmons, D. A. *Mass Spectrom. Rev.* **2003**, *22*, 1–26.
- (3) (a) Hoofnagle, A. N.; Resing, K. A.; Ahn, N. G. *Annu. Rev. Biophys. Biomol. Struct.* **2003**, *32*, 1–25. (b) Engen, J. R.; Smith, D. L. *Methods Mol. Biol.* **2000**, *146*, 95–112.
- (4) Wang, Y.; Gross, M. L. In *Applied Electrospray Mass Spectrometry*; Ganguly, A. K., Pramanik, B. N., Gross, M. L., Eds.; Marcel Dekker: New York, 2002; pp 389–410.
- (5) An exchange reaction is correlated if a number of otherwise protected amide hydrogens become transiently simultaneously solvated and thereby undergoes exchange. For example, a cooperative unfolding of a protein may lead to correlated exchange if the lifetime of the unfolded state is sufficiently long to allow exchange of several amide hydrogens.
- (6) Canet, D.; Last, A. M.; Tito, P.; Sunde, M.; Spencer, A.; Archer, D. B.; Redfield, C.; Robinson, C. V.; Dobson, C. M. *Nat. Struct. Biol.* **2002**, *9*, 308–315.
- (7) Engen, J. R.; Smithgall, T. E.; Gmeiner, W. H.; Smith, D. L. *Biochemistry* **1997**, *36*, 14384–14391.
- (8) Arrington, C. B.; Teesch, L. M.; Robertson, A. D. *J. Mol. Biol.* **1999**, *285*, 1265–1275.

- (9) Heegaard, N. H. H.; Jørgensen, T. J. D.; Rozlosnik, N.; Corlin, D. B.; Pedersen, J. S.; Tempesta, A. G.; Roepstorff, P.; Bauer, R.; Nissen, M. H. *Biochemistry*, in press.
- (10) Miranker, A.; Robinson, C. V.; Radford, S. E.; Aplin, R. T.; Dobson, C. M. *Science* **1993**, *262*, 896–900.
- (11) Jørgensen, T. J. D.; Gårdsvoll, H.; Danø, K.; Roepstorff, P.; Ploug, M. *Biochemistry* **2004**, *43*, 15044–15057.
- (12) Zhang, Z.; Smith, D. L. *Protein Sci.* **1993**, *2*, 522–531.

residue amide resolution. It is, however, imperative for the applicability of this method that no amide hydrogen is undergoing intramolecular migration (i.e., scrambling) in the gaseous peptide ion prior to dissociation. Significant hydrogen scrambling would evidently compromise any information gained from deuteration levels of fragment ions. Recently Deng et al.¹³ and Kim et al.^{14,15} have reported that levels of deuteration of amide groups in b-fragment ions generated by collision-induced dissociation (CID) of protonated peptides, obtained from pepsin digestion of deuterated proteins, were qualitatively correlated with amide hydrogen exchange rates obtained by NMR. However, the deuterium levels of y-fragment ions did not exhibit such a correlation indicating that scrambling had indeed occurred in the process of y-ion formation. Notwithstanding this, other CID studies of protonated proteins or peptides have reported that scrambling was also minor or negligible for y-ions.^{16–19} In contrast, both Demmers et al.²⁰ and Johnson et al.²¹ found that collisional activation of protonated peptides caused extensive scrambling of amide hydrogens in both b- and y-fragment ions. In agreement, other studies have demonstrated high mobility of amide hydrogens in collisionally activated peptides^{22,23} and a protein.²⁴ Until the pending controversy has been settled in the literature interpretation of deuterium levels of fragment ions must be evaluated with the appropriate precaution. It is thus imperative for this method to clarify which conditions cause scrambling of protonated peptides and to establish the causality for the observed amide hydrogen scrambling.

We have therefore undertaken a study of the hydrogen migration processes in protonated peptides upon collision-induced dissociation. Our peptides represent a uniquely controlled model system for the investigation of hydrogen scrambling processes due to the generation of regioselectively deuterium-labeled peptides. We can thus selectively deuterate either the C-terminal half or N-terminal half of these peptides by initiating isotopic exchange when the peptides are tightly bound to a soluble protein receptor; the urokinase-type plasminogen activator receptor (uPAR).²⁵ The C-terminal region of the peptides harbors the uPAR-binding sequence, which consequently gains protection against amide hydrogen exchange upon receptor binding. By contrast, the N-terminal half of the peptide is not involved in uPAR binding, and the direct exposure to the solvent ensures very rapid isotopic exchange. Initiation of amide ¹H/²H exchange by dilution of deuterated uPAR-peptide complexes into protiated buffer thus cause the unprotected (i.e., solvated) amide groups in the N-terminal half of

the peptide to become rapidly protiated, whereas those in the C-terminal half retain their deuterium (²H) due to the fact that they are shielded from the solvent by their engagement in receptor binding. Consequently, the b-ions encompassing the nonbinding region (i.e., the N-terminal region) constitute a very sensitive probe for detection of intramolecular migration involving amide hydrogens. If scrambling is negligible, these b-ions should contain ~0 deuterons, whereas the onset of scrambling can be readily monitored by an increasing amount of deuterium incorporation.

Experimental Section

Materials. D₂O (99.9 atom % D) was obtained from Cambridge Isotope Laboratories (Andover, MA), and ammonium acetate-*d*₇ (98 atom % D) was from Aldrich Chemicals. Pepsin immobilized on 6% agarose was obtained from Pierce (Rockford, IL). All other chemicals and reagents were of the highest grade commercially available. Peptides were synthesized, purified, and characterized as reported previously.^{25,26} Soluble, recombinant human uPAR was produced in CHO-cells and immunoaffinity purified as described previously.²⁷

Hydrogen/Deuterium Exchange. Deuterated uPAR was prepared by dissolving lyophilized protiated uPAR in deuterated buffer (50 mM *d*₇-ammonium acetate, pH 8.0 uncorrected value). After 12 h of deuteration at 6 °C, the sample was lyophilized and subsequently redissolved in deuterated buffer (50 mM *d*₇-ammonium acetate, pH 8.0 uncorrected value, 0.10 M NaCl). Deuterated peptide ligands were prepared in a similar manner. Deuterated uPAR-peptide complexes were formed by mixing a 2-fold molar excess of deuterated uPAR with deuterated peptide ligand.

Peptide ligands selectively labeled with deuterium in their uPAR binding region were prepared by a 50-fold dilution of a solution of deuterated uPAR-peptide complexes into protiated buffer (i.e., exchange-out): 1 μL of a 200 μM solution of the peptide ligand in the presence of 400 μM uPAR in deuterated buffer (50 mM *d*₇-ammonium acetate, pH 8.0, 0.10 M NaCl) was added to 49 μL of the corresponding protiated buffer (i.e., 50 mM ammonium acetate buffer, pH 8.0, 0.10 M NaCl). To prepare peptides labeled with deuterium in their nonbinding region, solutions of protiated uPAR-peptide complexes were diluted 50-fold into deuterated buffer (i.e., exchange-in). Solutions were maintained at 0 °C and subjected to exchange for 30 s. The ¹H/²H exchange solution was quenched by the addition of an equal volume of 0.5 M phosphate buffer (pH 2.2) and immediately frozen in liquid N₂. The samples were stored in liquid N₂ until analysis.

Rapid Desalting and ESI-MS-MS Analysis. The equipment for rapid desalting has previously been described.¹¹ Briefly, it consists of two HPLC pumps (Applied Biosystems Model 140B), an injection valve (Rheodyne Model 7725i), and a computer controlled 10-port two-position valve (Valco Model C2-1000A) equipped with a self-packed C₁₈ microcolumn. One HPLC pump delivered the solvent for desalting, and the other, for elution. Quenched samples were thawed individually and injected by an ice-cold HPLC syringe into a stainless steel loop mounted on the injection valve. For the pepsin digestion experiments the sample loop was replaced by a self-packed column with immobilized pepsin (Upchurch Omega column, 3 × 50 mm). Thus, digestion begins when the sample is loaded. When the handle of the injection valve is turned to the inject position the sample is flushed from the loop/pepsin column and desalted on the microcolumn with a flow of H₂O containing 0.05% (v/v) trifluoroacetic acid (pH 2.2). The sample was digested for 2 min in the column with immobilized pepsin and subsequently desalted for 3 min at 250 μL/min. With the stainless steel loop, the desalting time was 45 s at 400 μL/min. When the desalting time has elapsed,

- (13) Deng, Y. Z.; Pan, H.; Smith, D. L. *J. Am. Chem. Soc.* **1999**, *121*, 1966–1967.
- (14) Kim, M. Y.; Maier, C. S.; Reed, D. J.; Deinzer, M. L. *J. Am. Chem. Soc.* **2001**, *123*, 9860–9866.
- (15) Kim, M. Y.; Maier, C. S.; Reed, D. J.; Ho, P. S.; Deinzer, M. L. *Biochemistry* **2001**, *40*, 14413–14421.
- (16) Akashi, S.; Naito, Y.; Takio, K. *Anal. Chem.* **1999**, *71*, 4974–4980.
- (17) Waring, A. J.; Mobley, P. W.; Gordon, L. M. *Proteins* **1998**, *38*, 38–49.
- (18) Eyles, S. J.; Speir, J. P.; Kruppa, G. H.; Gierasch, L. M.; Kaltashov, I. A. *J. Am. Chem. Soc.* **2000**, *122*, 495–500.
- (19) Hoerner, J. K.; Xiao, H.; Dobo, A.; Kaltashov, I. A. *J. Am. Chem. Soc.* **2004**, *126*, 7709–7717.
- (20) Demmers, J. A. A.; Rijkers, D. T. S.; Haverkamp, J.; Killian, J. A.; Heck, A. J. R. *J. Am. Chem. Soc.* **2002**, *124*, 11191–11198.
- (21) Johnson, R. S.; Krylov, D.; Walsh, K. A. *J. Mass Spectrom.* **1995**, *30*, 386–387.
- (22) Harrison, A. G.; Yalcin, T. *Int. J. Mass Spectrom.* **1997**, *165*, 339–347.
- (23) Mueller, D. R.; Eckersley, M.; Richter, W. J. *Org. Mass Spectrom.* **1988**, *23*, 217–222.
- (24) McLafferty, F. W.; Guan, Z. Q.; Haupts, U.; Wood, T. D.; Kelleher, N. L. *J. Am. Chem. Soc.* **1998**, *120*, 4732–4740.
- (25) Ploug, M.; Østergaard, S.; Gårdsvoll, H.; Kovalski, K.; Holst-Hansen, C.; Holm, A.; Ossowski, L.; Danø, K. *Biochemistry* **2001**, *40*, 12157–12168.

- (26) Ploug, M.; Østergaard, S.; Hansen, L. B.; Holm, A.; Danø, K. *Biochemistry* **1998**, *37*, 3612–3622.
- (27) Ploug, M.; Kjalke, M.; Rønne, E.; Weidle, U.; Høyer-Hansen, G.; Danø, K. *J. Biol. Chem.* **1993**, *268*, 17539–17546.

the Valco valve automatically switches and the sample is eluted directly into the electrospray ion source with a flow of 70% (v/v) acetonitrile containing 0.05% (v/v) trifluoroacetic acid at 20 μ L/min. The solvent precooling coils, Rheodyne injector with loop, and the Valco 10-port valve with microcolumn were immersed in an ice/water slurry (0 °C) to minimize back-exchange with the protiated solvents. The desalting step removes deuterium incorporated into side chains and amino/carboxy termini, since these labile hydrogens (i.e., hydrogen attached to N, O and S) exchange much faster than peptide backbone amide hydrogens at acidic pH.²⁸ Thus, the mass increase observed after deuteration and desalting reflect primarily deuterium incorporation at the main chain amide groups.

Positive ion ESI mass spectra and CID spectra were acquired on Micromass quadrupole time-of-flight mass spectrometers (Q-TOF 1 and Q-TOF Ultima) equipped with electrospray ion sources. The instruments were calibrated using sodium iodide. The ion source parameters for the Q-TOF 1 were as follows: capillary voltage 3.1 kV, cone voltage 45 V, ion source block temperature 60 °C, nebulizer gas flow 20 L/h (25 °C), desolvation gas flow 400 L/h (200 °C). Nitrogen was used as nebulizer and desolvation gas. For the Q-TOF Ultima the source block temperature was 80 °C, cone voltage, 100 V, and ion tunnel one, 40 V; otherwise, similar electrospray parameters were used. Note that the ion transfer optics in the first stages of the Q-TOF Ultima mass spectrometer is different from that of the Q-TOF 1. All spectra shown in the present work were obtained with the Q-TOF Ultima. In the collision-induced dissociation (CID) experiments, the isotopic envelopes of the regioselectively labeled peptides were transmitted by the quadrupole (LH = HM = 8) and then accelerated into the hexapole collision cell. The laboratory collision energies for doubly protonated AE138 and AE133 were 42 and 64 eV, respectively. Argon was used as a collision gas at an indicated manifold pressure of 9×10^{-5} mBar (note that the pressure is not measured directly in the CID collision chamber). The product ions formed by the internal excitation and subsequent dissociation of the parent ions were then mass analyzed by the orthogonal TOF analyzer. To obtain good fragment ion statistics, four separate injections of selectively labeled peptides were accumulated in each CID spectrum (signal-to-noise ratio for the weakest diagnostic fragment ion was better than 15). The assignment of fragment ions was confirmed by CID of N-terminal acetylated AE138 and AE133. All b-ions displayed a mass shift of 42 Da.

The incubation of uPAR·AE138 complexes in exchange buffer yielded distinct bimodal isotope distributions. In deuterium exchange-in experiments, the lower-mass population of this bimodal isotope distribution was selected for CID experiments because only this population is selectively labeled. In deuterium exchange-out experiments, the higher-mass population was selectively labeled, and therefore it was subjected to CID. The relative slow dissociation rates of the uPAR·peptide complexes employed in the present study and the short labeling period (~30 s) ensure that a high proportion of selectively labeled peptides are available for CID experiments.

Data Analysis

The deuterium content of peptide ions and their fragments was determined from the difference between the average mass of the deuterated peptide and the average mass of the corresponding fully protiated peptide. The average masses were determined from centroided isotopic distributions exported into a spreadsheet using nominal masses. The deuterium incorporation distributions were obtained by deconvolving the isotope natural abundance distribution from mass spectra of deuterium-labeled peptides using the maximum entropy method in the HXpro software kindly provided by Dr. Z. Zhang.²⁹ Exchange rates for unligated peptides at quench conditions were calculated

Table 1

ligand	sequence ^a	ΔD^b	D^c	k_{off}^d
AE105	D-Cha-FsrYLWS	5.8	7	1.2
AE133	KGSGG-D-Cha-FsrYLWS	6.5	7	0.9
AE138	KGSGG-D-Cha-FsaYLWS	6.5	7	6.3

^a Amino acids are shown in the single letter code where capitals denote L-chirality and lower case D-chirality. Peptides have unmodified N- and C-termini. Cha is β -cyclohexyl-(L)-alanine. ^b Minimum number of protected amide hydrogens. This number is derived from the difference in average masses of peptides obtained from deuterium exchange-out experiments (30 s protiation) in the presence or absence of a 2-fold molar excess of uPAR. ^c Exact number of protected amide hydrogens as determined from the deuterium distributions of peptides obtained from deuterium exchange-out experiments (30 s protiation) in the presence of a 2-fold molar excess of uPAR. ^d Dissociation rate constants, $k_{\text{off}} \times [10^{-4} \text{ s}^{-1}]$, were measured by amide hydrogen exchange for uPAR^{wt}.¹¹

with the SPHERE software (available at <http://www.fccc.edu/research/labs/roder/sphere/>).

To calculate the theoretical deuterium content of the fragment ions in the case of 100% scrambling, the deuterium fraction of the precursor ion, F_D , was determined. F_D is given by $P_{(D)}/N_H$, where $P_{(D)}$ is the experimental deuterium content of the precursor ion and N_H is the total number of hydrogens assumed to participate in the scrambling process (i.e., labile hydrogens). The theoretical deuterium content of the fragment ions was then determined by multiplying the number of labile hydrogens in the fragments with the deuterium fraction of the precursor. To investigate whether certain types of hydrogens were excluded from the scrambling process a hydrogen atom inventory was made containing the number of each type of N- and O-linked hydrogen atoms (i.e., amino, amide, carboxy, hydroxy, indole, and phenoxy) in the precursor and fragment ions. A given type of hydrogen was excluded from the scrambling process by not including this particular type in the number of labile hydrogens when calculating F_D and the theoretical D content of the fragment ions.

Results

A number of peptides that binds to and antagonize the function of the urokinase-type plasminogen activator receptor (uPAR) have recently been developed by a combination of phage-display technology, affinity maturation by combinatorial chemistry, and affinity measurements by surface plasmon resonance.³⁰ We have previously shown that at least six out of a total of eight amide hydrogens in the peptide AE105 (D-Cha-FsrYLWS) are efficiently protected against exchange when it forms a tight complex with uPAR ($K_d < 1 \text{ nM}$).¹¹ To enable the preparation of peptides having the unique property of being regioselectively labeled with deuterium, we have synthesized two extended analogues of the nonamer AE105: AE133 and AE138. These analogues are 14-mer peptides harboring a uPAR binding sequence as well as a N-terminal nonbinding sequence extension (see Table 1). The amide hydrogens in the uPAR binding sequence are engaged in stable hydrogen bonding when bound to uPAR and these particular hydrogens are thus protected against exchange with the solvent. By contrast, amide hydrogens residing in the nonbinding sequence are continuously solvated (i.e. unprotected) and consequently rapidly exchanged. This unique property enables us to label AE138 and AE133 with

(29) Zhang, Z. Q.; Guan, S. H.; Marshall, A. G. *J. Am. Soc. Mass Spectrom.* **1997**, *8*, 659–670.

(30) Ploug, M. *Curr. Pharm. Des.* **2003**, *9*, 639–652.

(28) Bai, Y.; Milne, J. S.; Mayne, L.; Englander, S. W. **1993**, *17*, 75–86.

deuterium exclusively in their uPAR binding region. This is accomplished by initiating $^1\text{H}/^2\text{H}$ exchange by dilution of deuterated uPAR·peptide complexes into protiated buffer (i.e., representing a deuterium *exchange-out* experiment). The protected amide hydrogens in the uPAR binding sequence retain their deuterium, whereas the unprotected (i.e., solvated) amide groups become protiated. To obtain the reciprocal deuteration pattern of the peptides $^1\text{H}/^2\text{H}$, exchange is merely initiated by diluting protiated uPAR·peptide complexes into deuterated buffer (i.e., representing a deuterium *exchange-in* experiment). In a previous study, we determined the minimum number of protected amide hydrogens in peptides bound to uPAR by such exchange-in experiments.¹¹ Determination of the exact number of protected amide hydrogens by this approach is, however, hampered by slow exchange reactions occurring under quench conditions causing erroneous deuterium loss or gain.¹¹ As addressed in the next paragraph we now demonstrate by deuterium *exchange-out* experiments that exactly seven amide hydrogens are protected in all these peptides irrespective of their chain length (Table 1) when they participate in uPAR complexes.

Determination of the Exact Number of Amide Hydrogens in the Peptide Ligand AE105 That Become Protected Due to Its Interaction with uPAR. Figure 1 shows mass spectra of doubly protonated AE105 derived from deuterium exchange-out experiments in the presence or absence of uPAR. Without uPAR, predeuterated AE105 exchanges all of its amide deuterons with protons within 30 s of incubation in protiated buffer at pH 8.0 (compare Figure 1C and D). The low average deuterium content after exchange (~ 0.3) reflects the residual amount of D atoms in the exchange buffer. None of the amide hydrogens in uncomplexed AE105 are thus protected against exchange with the solvent. As opposed to this, the presence of uPAR increases the average deuterium content of AE105 to 6.1 after 30 s of protiation (Figure 1A). The average mass difference between the isotopic distributions of AE105 acquired after 30 s of exchange-out in the presence or absence of uPAR is 5.8 (Figure 1A and C), which is identical to the value obtained in a previous exchange-in experiment.¹¹ The mass difference of 5.8 demonstrates that six or more amide hydrogens are protected against exchange in receptor-bound AE105. To obtain a more accurate estimation on the total number of protected amide hydrogens, we calculated the deuterium incorporation distribution for AE105 bound to uPAR. This distribution reveals that $\sim 30\%$ of the population has retained a maximum of seven deuterons (Figure 1E). This provides direct evidence for the protection of seven amide hydrogens upon complexation with uPAR. The deuterium distribution also shows that a significant proportion of the molecules has retained six or fewer deuterons. This is caused by the unavoidable loss of deuterium that occurs during the quenching conditions, which affects the N-terminal amide hydrogen in particular as its exchange rate is accelerated by the proximal cationic charge of the N-terminal ammonium ion.²⁸ The deuterium loss caused by back-exchange under quench conditions was 12% for fully deuterated AE105. This number was obtained from experiments where deuterated AE105 was diluted directly (1:50) into cold quench buffer and subjected to desalting followed by mass spectrometric analysis (data not shown). Similar values were obtained for AE133 and AE138.

A distinct bimodal isotope distribution is evident upon prolonged incubation of uPAR·AE105 complexes in protiated

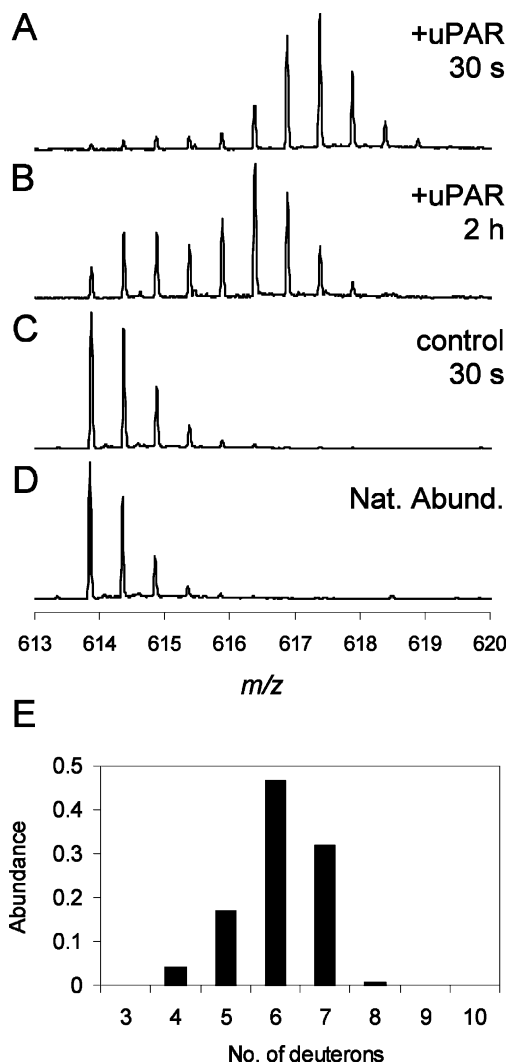


Figure 1. Amide $^1\text{H}/^2\text{H}$ exchange on AE105 (D-Cha-FsrYLWS) in the presence (A,B) or absence (C) of uPAR. Shown are ESI mass spectra of $[\text{AE105} + 2\text{H}]^{2+}$ obtained after deuterium exchange-out for 30 s (A,C) and 2 h (B). Spectrum D shows the natural abundance isotopic distribution. The deuterium incorporation distribution of spectrum A is shown in part E.

buffer (Figure 1B). Such a bimodal distribution is a signature of a correlated exchange mechanism,^{7,8,11} indicating that a number of otherwise protected amide hydrogens become simultaneously solvated and hence exchange rapidly. In our case, correlated exchange occurs whenever uPAR·AE105 complexes dissociate and previously protected amide hydrogens on AE105 are exposed to the solvent. This results in nearly complete exchange of these amide hydrogens before AE105 reassociates with uPAR.¹¹ The low-mass envelope of isotope peaks in Figure 1B corresponds to such a population of AE105 molecules that has been dissociated from uPAR and thereby undergone correlated exchange, whereas the high-mass envelope corresponds to a population of molecules that have remained bound to the receptor.

Preparation of Regioselectively Deuterium Labeled Peptides. AE133 is an extended analogue of AE105 with five additional amide hydrogens located in the N-terminus, and as they do not contribute to the interface of the interaction, they are not protected from exchange in the uPAR complex. This property is clearly illustrated by the calculated deuterium

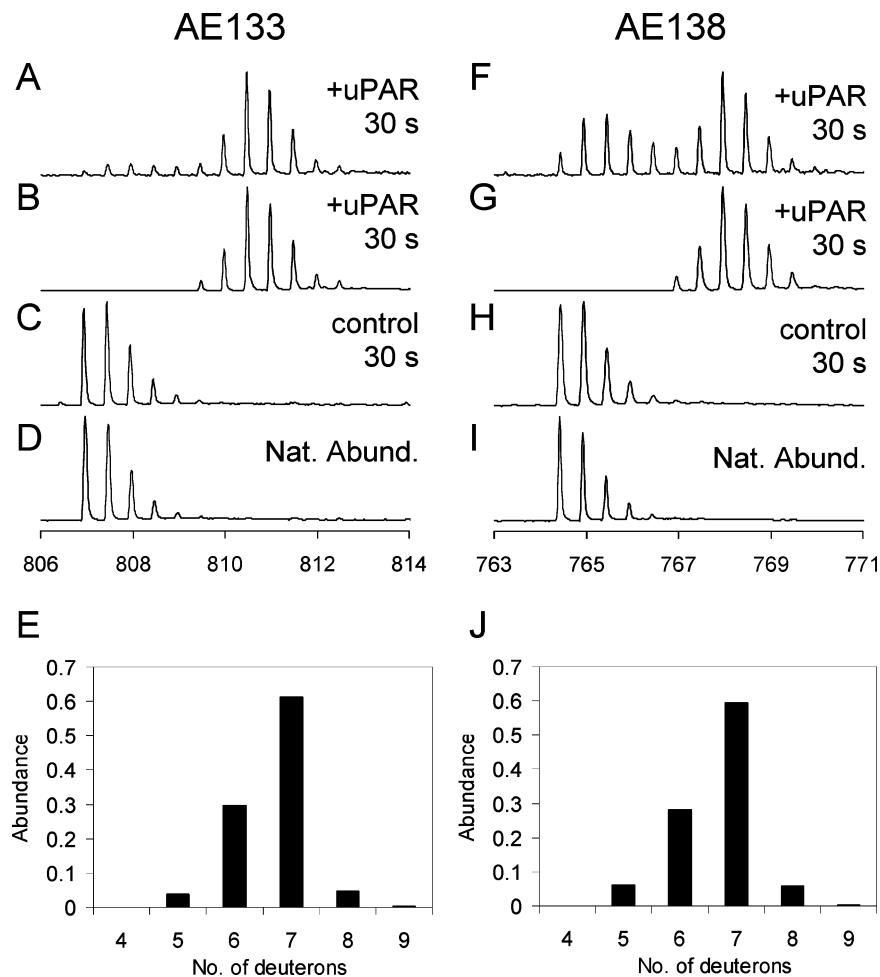


Figure 2. Amide $^1\text{H}/^2\text{H}$ exchange on AE133 (KGSGGD-Cha-FsrYLWS; left column) and AE138 (KGSGGD-Cha-FsaYLWS; right column) in the presence (A,B,F,G) or absence (C,H) of uPAR. Shown are ESI mass spectra of doubly protonated peptides obtained after deuterium exchange-out for 30 s. Mass selected precursor ions for CID experiments are shown in spectra B and G. Spectra D and I show the natural abundance isotopic distributions. The deuterium incorporation distributions of spectra B and G are shown in parts E and J.

distribution for AE133 (Figure 2E) that is derived from an experiment in which uPAR·AE133 complexes are incubated in protiated buffer for 30 s (Figure 2A). As the dominating peptide population ($\sim 61\%$) has retained seven deuterons (Figure 2E), this shows that seven amide hydrogens in AE133 are protected against exchange as a result of its interaction with uPAR and this reassuringly replicates exactly the protection pattern observed for the shorter parent peptide AE105. As expected the remaining six amide hydrogens in the nonbinding region of AE133 are in rapid isotopic exchange with the buffer containing 2% residual deuterium. This leads to a nonspecific incorporation level corresponding to a single deuterium in this region for theoretically $6 \times 0.02 \times 0.61 = 7\%$ of the molecules, which is in good agreement with the experimental observation of a minor population $\sim 5\%$ harboring eight deuterons.

AE138 differs from AE133 by a single arginine to alanine substitution in the uPAR binding sequence which provides AE138 with a higher dissociation rate.¹¹ This feature accentuates the formation of a distinct bimodal isotope distribution when deuterated uPAR·AE138 complexes are incubated in protiated buffer for 30 s (Figure 2F) as compared to the stable uPAR·AE133 complexes (Figure 2A). However, the high-mass envelopes, representing the populations of molecules that have remained bound to the receptor during the exchange period, are almost indistinguishable between AE133 and AE138 (compare

deuterium distributions in Figure 2E and 2J). To identify the seven protected sites in the uPAR binding sequence of AE138, deuterated uPAR·AE138 complexes were incubated in protiated buffer for 30 s and subsequently fragmented by pepsin after acid quenching (Figure 3). Importantly, pepsin cleavage divides AE138 into a C-terminal fragment (FsaYLWS) harboring the receptor binding site and the corresponding nonbinding N-terminal fragment (KGSGGD-Cha). In accordance, the C-terminal fragment retains a maximum of five deuterons (Figure 3H), while the N-terminal fragment contains only a negligible amount of deuterium (Figure 3I). Since intact AE138 retains a maximum of seven deuterons, the pepsin cleavage per se has caused the loss of two deuterons. This is most likely accounted for by the enzymatic conversion of the scissile amide group of Phe (F) into an amino group, which is in very rapid exchange with the solvent at low pH. Another consequence of this cleavage is the formation of the positive charge of the α -amino group at Phe, which accelerates the exchange rate of the adjacent Ser amide hydrogen ~ 14 -fold at quench conditions. Note, the C-terminal COOH group in KGSGGD-Cha does not accelerate the exchange rate of the Cha amide hydrogen.³¹ Furthermore, the average deuterium content of protected FsaYLWS (4.5) was found to be in excellent agreement with the theoretical deuterium content (4.8) calculated for a back-exchange time of 6 min and assuming an initial deuterium content of 6. Along the same line

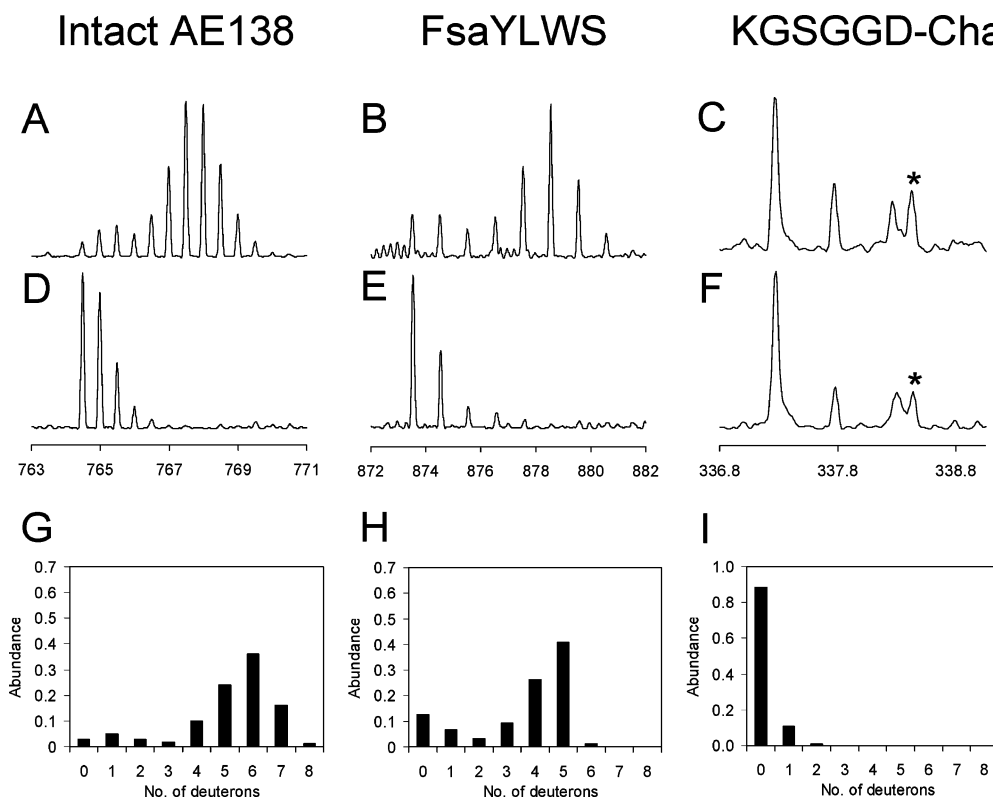


Figure 3. Mass spectra obtained from a pepsin digestion of fully deuterated uPAR·AE138 (A,B,C) or fully protiated uPAR·AE138 (D,E,F) incubated in protiated buffer at pH 8.0 for 30 s prior to digestion by pepsin at pH 2.2. The deuterium incorporation distributions of spectra A, B, and C are shown in parts G, H, and I. Asterisked peaks are not part of the isotopic envelope of the N-terminal fragment.

of evidence, we find that the theoretical deuterium content of KGSGGD-Cha assuming no residues are protected (0.09) is indistinguishable from that determined experimentally (0.11). In conclusion, the finding of five deuterons in FsaYLWS and virtually none in KGSGGD-Cha proves that the seven C-terminally positioned amide hydrogens in AE138 (i.e., -FsaYLWS) become protected upon binding to uPAR.

Collision-Induced Dissociation of Regioselectively Deuterium Labeled Peptides. Collision-induced dissociation of doubly protonated AE138 yields a nice series of b-fragment ions (b_6 , b_8 , b_9 , b_{10} , b_{11} , b_{12} , and b_{13}) (Figure 4A). This abundant b-ion series results from the presence of the N-terminal Lys residue in AE138. The deuterium content of these b-fragment ions generated by CID of AE138 are shown in Figure 5, which discriminates between deuterium labeling in either the uPAR binding region (Figure 5A) or in the nonbinding region (Figure 5B). Also shown in Figure 5 is the theoretical deuterium content of these ions assuming either 0% or 100% scrambling between all N- and O-linked hydrogens or the N-linked hydrogens only. The interpretation of this experiment is exemplified by the b_6 -ion, which is located outside the receptor-binding region. Notably, the experimental deuterium content of this b_6 -ion is 2.8, when it is derived from AE138 selectively labeled with deuterons in uPAR binding region. Assuming 0% scrambling the theoretical deuterium content of the b_6 -ion should be close to zero under these conditions. This is obviously not the case and the experimentally determined value of 2.8 corresponds on the contrary almost exactly to the theoretical D content of 2.9,

which is calculated for the b_6 -ion assuming 100% scrambling between all N- and O-linked hydrogens. A similar good agreement between experimental and theoretical values for 100% scrambling is observed for the entire b-ion series. In quantitative terms, the deviation is only $\chi^2_{100\%} = 0.08$, while the correlation between experimental data and theoretical values for 0% scrambling is very poor ($\chi^2_{0\%} = 5.1$). Concordantly, the deuterium content of the b-ion series generated from AE138 labeled with deuterons at its nonbinding region also exhibits a very good agreement with the theoretical values for 100% scrambling, as shown in Figure 5B ($\chi^2_{100\%} = 0.04$ vs $\chi^2_{0\%} = 6.1$). In particular, the nonlinear (stepwise) increments in the experimental D content with increasing b-ion size are remarkably well described by the scrambling model with 100% randomization between all N- and O-linked hydrogens. If, however, O-linked hydrogens were not included in the scrambling mechanism, the D content would increase linearly from b_6 to b_{12} . This linearity is a consequence of each residue within this particular series having exactly one N-linked hydrogen (i.e., the amide hydrogen). Deviation from linearity occurs in the theoretical deuterium content when a difference in the number of labile hydrogens between the involved residues exists. The nearly perfect agreement between the experimental data and the theoretical values for 100% scrambling proves that complete randomization of all N- and O-linked hydrogens has occurred prior to or during dissociation of AE138.

The CID spectrum of doubly protonated AE133 is markedly different from that of AE138 (compare Figure 4A and Figure 4B). Only three abundant b-ions are observed (b_6 , b_{12} , and b_{13}). Furthermore, higher collision energy is required to induce

(31) The effect of the C-terminal COOH group on the amide hydrogen exchange rate in Cha was investigated by mimicking Cha with either Phe or Ile. For both residues, the effect was negligible.

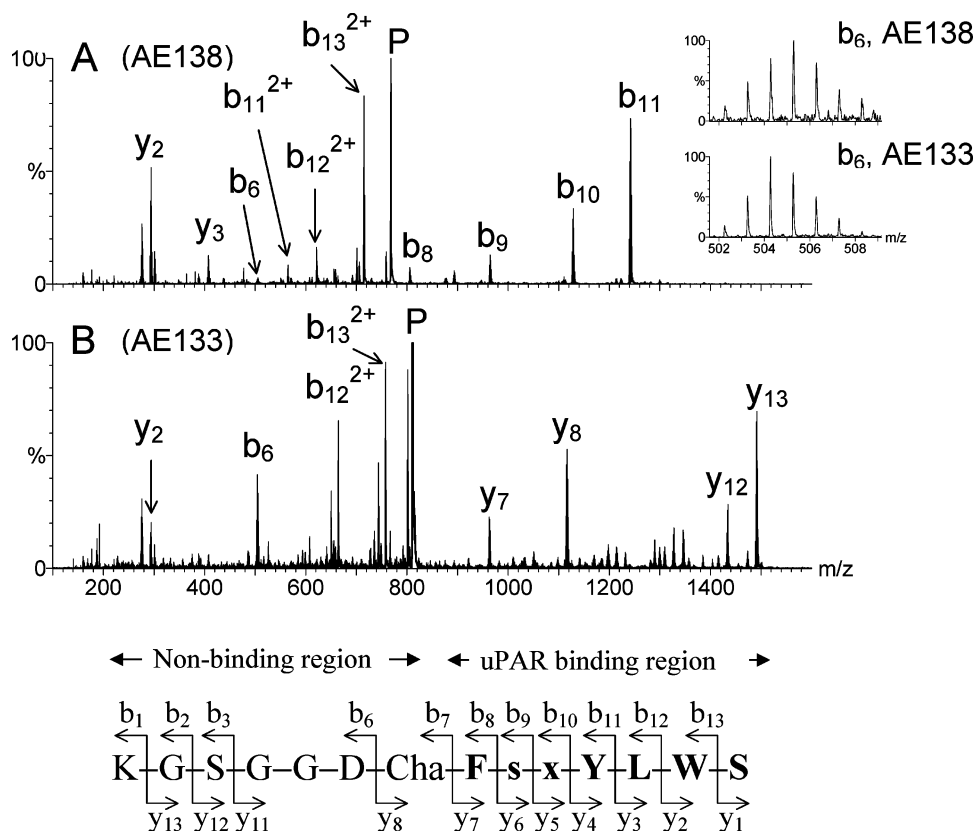


Figure 4. CID spectra of doubly protonated AE138 (A) and AE133 (B) labeled with deuterium in their uPAR binding sequence. Precursor ions are labeled P. Insert shows the isotopic distributions of their b_6 -fragment ions. The fragmentation scheme shows sequences of the fragment ions, x = (D)-Ala and (D)-Arg for AE138 and AE133, respectively. Cha is cyclohexyl-(L)-alanine. Lower case single letter code denotes D-chirality of amino acid residue.

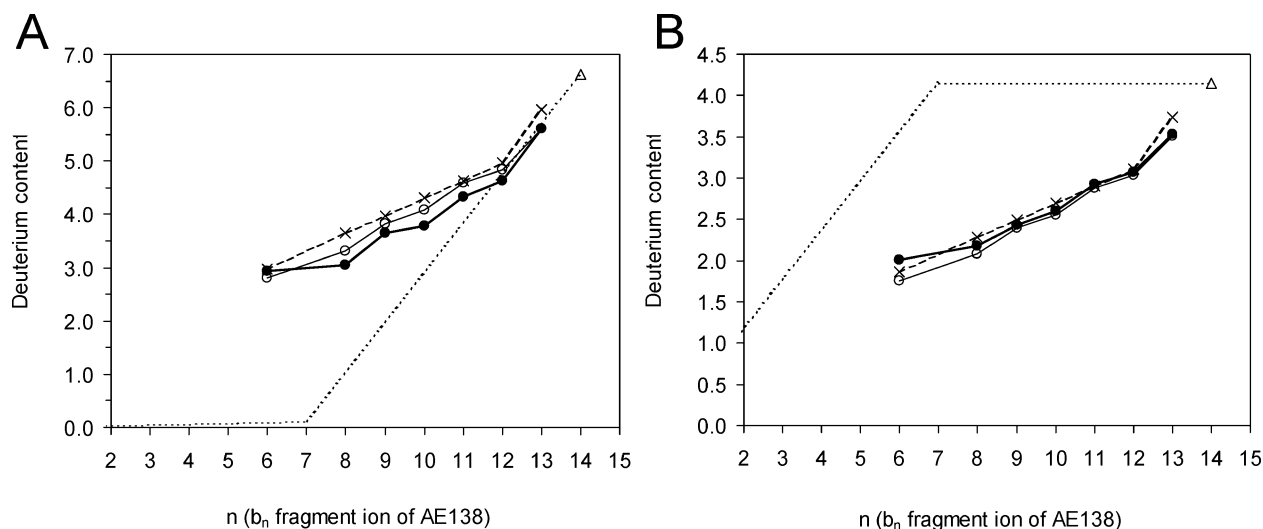


Figure 5. Deuterium content of b_n -fragment ions (filled circles, thick line) generated by CID of doubly protonated AE138 labeled with deuterium in either the uPAR binding region (A) or the nonbinding region (B). The dotted lines indicate the theoretical deuterium content in case of 0% scrambling. Also shown is the theoretical deuterium content of b_n -fragment ions in case of 100% scrambling between all hydrogens attached to nitrogen and oxygen (open circles, thin line) or excluding O-linked hydrogens from the scrambling process (crosses, dashed line). The open triangles indicate the deuterium content of the precursor ions.

fragmentation of AE133 compared to AE138 ($E_{\text{LAB}} = 64$ and 42 eV, respectively). This difference is accounted for by the fact that AE133 contains two residues with high gas phase proton affinity (Lys and Arg), whereas AE138 only contains one such residue (Lys). If the number of charges (protons) is equal to or less than the number of residues with high proton affinity, more internal energy is required to effect fragmentation.³² In addition, the fragmentation pattern is known to be

strongly influenced by the presence of Arg.^{32a,33} Thus, the presence of arginine in diprotonated AE133 increases the dissociation threshold relative to AE138 and changes the

- (32) (a) Dongre, A. R.; Jones, J. L.; Somogyi, A.; Wysocki, V. H. *J. Am. Chem. Soc.* **1996**, *118*, 8365–8374. (b) Tsapralis, G.; Nair, H.; Somogyi, A.; Wysocki, V. H.; Zhong, W. Q.; Futrell, J. H.; Summerfield, S. G.; Gaskell, S. J. *J. Am. Chem. Soc.* **1999**, *121*, 5142–5154.
 (33) Tabb, D. L.; Huang, Y. Y.; Wysocki, V. H.; Yates, J. R. *Anal. Chem.* **2004**, *76*, 1243–1248.

fragmentation pattern. As the b_6 -ion of AE133 is encompassed by the nonbinding region, it represents an ideal diagnostic fragment ion for probing the degree of scrambling in AE133. An observed deuterium content of 2.3 for this b_6 -ion of AE133 is nicely predicted by a model involving 100% scrambling (2.4), as was also the case for AE138. An abundant y_8 -ion, being complementary to the b_6 -ion, is also present in the CID spectrum of AE133. The deuterium content of this y_8 -ion is 4.2, which is identical to the theoretical content in case of 100% scrambling. As a matter of curiosity, the b_6 -ion from AE133 contains less deuterium than the corresponding b_6 -ion from AE138 despite the fact that the precursors (i.e., AE138 and AE133) have similar deuterium content. This difference is, however, caused by AE133 having a lower deuterium fraction than AE138 (0.225 vs 0.255), since AE133 in the uPAR-binding region contains four additional hydrogens participating in intramolecular migration due to the introduction of the guanido group (Ala to Arg substitution). In accordance with the previous experiments, the deuterium content of the b_6 - and y_8 -ions generated from CID of AE133 selectively labeled with deuterium in the nonbinding region also mimics the theoretical values for 100% scrambling (data not shown).

Discussion

Comparison to Other H/D Exchange CID MS Studies. In recent years gas-phase fragmentation has been employed in the attempt to localize sites or segments within proteins or peptides that have incorporated deuterium during a solution $^1\text{H}/^2\text{H}$ exchange experiment.^{13–20,34–41} It is however mandatory for this method that no or at least negligible levels of intramolecular hydrogen atom migration (i.e., hydrogen scrambling) have occurred. Otherwise, interpretation of deuterium levels in fragment ions will not bear any relevance to the solution structure of the protein, and erroneous conclusions will inevitably be drawn. At present conflicting results exist in the literature as to the extent of hydrogen scrambling in protonated peptides and proteins upon gas phase collisional activation. Our results show that all N- and O-linked hydrogens in two doubly protonated peptides (AE138 and AE133) evidently undergo intramolecular hydrogen atom migration at such a high rate upon collisional activation that they lose their positional identity prior to peptide cleavage. Thus, the deuterium atoms that were initially located at specific amide groups in solution become statistically distributed over all exchangeable sites in the gaseous b- and y-fragment ions (i.e., complete scrambling has occurred). This finding is clearly contradictory to two recent studies in which the degree of hydrogen scrambling in b-ions was reported either to be negligible¹³ or to occur at a low level.¹⁴ Notwithstanding these findings, Demmers et al.²⁰ demonstrated such a high degree of hydrogen scrambling in b-ions for a series of

protonated peptides that they precluded the use of CID to obtain site-specific deuteration levels. For the sake of completeness, it should be emphasized that differences in the experimental conditions among these studies exist. As such differences may affect the scrambling processes, we will consider them in more detail. Peptides investigated by Demmers et al.²⁰ were electrosprayed while they were embedded in phospholipid bilayers dispersed in deuterated buffer at pD 7.5. The present study as well as those of Deng et al.,¹³ Kim et al.¹⁴ electrosprayed peptides in cold acidic protiated $\text{H}_2\text{O}/\text{CH}_3\text{CN}$ solvent (i.e. the conventional method). It cannot be excluded that the conditions used by Demmers et al. may effect hydrogen scrambling during the ionization process. This precaution is however not needed in the present study, since there is a large molar excess of water protons relative to peptide deuterons during the process of desolvation in the charged micro droplets. If scrambling was to occur, it would inevitably deplete the deuterium content of the peptide ion as the water evaporated. The high deuterium content of our deuterated controls strongly argues against any significant deuterium depletion during evaporation from the microdroplet. Thus, it is most likely that it is the collisional activation process per se that initiates the intramolecular hydrogen migration reactions resulting in hydrogen scrambling. In the studies by Deng et al.¹³ and Kim et al.,¹⁴ the protonated peptides were collisionally activated in a quadrupole ion trap mass spectrometer, whereas our peptides were activated in a quadrupole time-of-flight mass spectrometer (Q-TOF). Related to this discussion Demmers et al.²⁰ observed extensive hydrogen scrambling in both a Q-TOF and an ion-trap mass spectrometer. Importantly, heating of precursor ions is slower in the ion trap compared to the Q-TOF as the activating collisions are less energetic in an ion trap resulting in a gradual accumulation of internal energy in the precursor ions on a longer time scale (10–100 ms vs ~ 0.1 ms).⁴² This difference in ion activation could be speculated to contribute to the observed differences. It is, however, widely accepted that the probability for intramolecular reactions in protonated peptides increases significantly with longer ion activation time.^{43–45} This relationship is emphasized by a recent study by Hoerner et al.,¹⁹ where a high degree of hydrogen scrambling was observed upon CID of protein ions using SORI (sustained off-resonance irradiation) during which the ion activation time typically is 0.1–1 s.⁴² Surprisingly, a low degree of scrambling was found upon CID of the same protein in the electrospray ion source (i.e., nozzle-skimmer fragmentation). The energetics of nozzle-skimmer fragmentation is similar to that of CID in the collision cell of a Q-TOF mass spectrometer (as used in the present study).^{42,46} Thus, the difference in the degrees of scrambling between our study and Hoerner et al.¹⁹ cannot be explained by differences in the ion activation method. The lower degree of scrambling as observed with nozzle-skimmer fragmentation appears to be related to a high number of intramolecular hydrogen bonds in the gaseous protein that inhibit the scrambling process.¹⁹ In the context of the “mobile proton” model for amide bond cleavage (vide infra),

(34) Yan, X. G.; Zhang, H. D.; Watson, J.; Schimerlik, M. I.; Deinzer, M. L. *Protein Sci.* **2002**, *11*, 2113–2124.

(35) Akashi, S.; Takio, K. *J. Am. Soc. Mass Spectrom.* **2001**, *12*, 1247–1253.

(36) Anderegg, R. J.; Wagner, D. S.; Stevenson, C. L.; Borchardt, R. T. *J. Am. Soc. Mass Spectrom.* **1994**, *5*, 425–433.

(37) Akashi, S.; Takio, K. *Protein Sci.* **2000**, *9*, 2497–2505.

(38) Buijs, J.; Hakansson, K.; Hagman, C.; Hakansson, P.; Oscarsson, S. *Rapid Commun. Mass Spectrom.* **2000**, *14*, 1751–1756.

(39) Kraus, M.; Janek, K.; Bienert, M.; Krause, E. *Rapid Commun. Mass Spectrom.* **2000**, *14*, 1094–1104.

(40) Yamada, N.; Suzuki, E.; Hirayama, K. *Rapid Commun. Mass Spectrom.* **2002**, *16*, 293–299.

(41) Kraus, M.; Bienert, M.; Krause, E. *Rapid Commun. Mass Spectrom.* **2003**, *17*, 222–228.

(42) McLuckey, S. A.; Goeringer, D. E. *J. Mass Spectrom.* **1997**, *32*, 461–474.

(43) Vachet, R. W.; Bishop, B. M.; Erickson, B. W.; Glush, G. L. *J. Am. Chem. Soc.* **1997**, *119*, 5481–5488.

(44) Yague, J.; Paradela, A.; Ramos, M.; Ogueta, S.; Marina, A.; Barahona, F.; de Castro, J. A. L.; Vazquez, J. *Anal. Chem.* **2003**, *75*, 1524–1535.

(45) Kaltashov, I. A.; Eyles, S. J. *J. Mass Spectrom.* **2002**, *37*, 557–565.

(46) Harrison, A. G. *Rapid Commun. Mass Spectrom.* **1999**, *13*, 1663–1670.

such an inhibition of proton-transfer reactions would be expected also to protect the polypeptide chain against cleavage, but this appears not to be the case. A problem associated with nozzle-skimmer fragmentation is, however, the risk of intermolecular gas-phase H/D exchange reactions with residual water/organic solvent vapor in the high-pressure region of the electrospray ion source. Using an ion source similar to that of Hoerner et al.,¹⁹ it was demonstrated by Hagman et al.⁴⁷ that fragment ions generated by nozzle-skimmer fragmentation exhibit very different degrees of gas phase reactivity with respect to intermolecular H/D exchange, and this may cause depletion of deuterium for certain fragment ions. Such reactions cannot occur in Q-TOF MS/MS experiments in which the precursor ion is mass-selected and collisionally activated in a collision cell filled with an inert gas.

Comparison to the “Mobile Proton Model” for Peptide Fragmentation. The occurrence of hydrogen scrambling observed in our experiments represents a logic chain of events for the hypothetical fragmentation mechanism proposed in “the mobile proton model”, which provides a plausible reaction mechanism for the formation of b- and y-fragment ions from protonated peptides. According to this model, the first step is an endothermic proton transfer from a site of higher proton affinity (e.g., the N-terminal amino group) to the amide nitrogen.^{32a,48} This reaction is facilitated by the increase in internal energy acquired by, e.g., collisions with a gas. Protonation of the amide nitrogen weakens the amide bond and decreases the electron density of the carbon atom of the amide group thereby making it a target for nucleophilic attack by the oxygen of the adjacent amide group. Attack of the adjacent oxygen and concomitant cleavage of the amide bond result in the formation of b-type ion with the protonated 2-substituted-5-oxazolone structure, while the y-fragment retains its linear peptide structure.^{49–53} Hydrogen scrambling will take place if amide nitrogens participate in the reversible proton-transfer reactions without amide bond cleavage (i.e., if protonated amide nitrogens readily back-transfer protons without the formation of fragment ions). Recent theoretical studies on protonated peptides have shown that proton transfer reactions between the energetically favored site and the amide nitrogen indeed occur at internal energies well below the lowest dissociation threshold energy.^{54–57} For example, triglycine protonated on the second amide nitrogen is 18.7 kcal/mol higher in free energy than the lowest energy structure, while the free energy barrier to generate

the b₂-ion is 32.5 kcal/mol as determined by high level density functional theory calculations.⁵⁷ Thus, the energy barrier for dissociation is substantially higher than that of amide nitrogen protonation thereby enabling scrambling processes in such protonated peptides upon collisional activation. Larger peptides such as those employed in this study are not amenable to high level ab initio calculations. The present study shows, however, that the deuterium atoms are statistically distributed over all possible exchangeable sites in b- and y-ions. All amide hydrogens as well as other N- and O-linked hydrogens have thus extensively participated in intramolecular proton/deuteron transfer reactions before cleavage of the amide bond. This experimental finding further substantiates the molecular mechanism provided by the mobile proton model for peptide fragmentation. Interestingly, enhanced cleavage of the Asp-Cha bond is observed upon CID of [AE133 + 2H]²⁺ (note the abundant complementary product ion pair, b₆/y₈, in Figure 4B). Such preferential cleavage adjacent to Asp residues has been explained by a mechanism in which the acidic proton of the Asp side chain initiates fragmentation by protonation of the amide nitrogen.^{32b} This selective cleavage is, however, only observed when the ionizing protons are sequestered by residues with a high proton affinity (i.e., when the number of basic residues exceeds or equals the number of ionizing protons).^{32b} In this situation, the protons are thought to exhibit reduced mobility, and only in this particular case will a selective cleavage at Asp residues be facilitated. In such a scenario, one might furthermore anticipate that reduced proton mobility would result in a low degree of hydrogen atom scrambling. However, the present data do not substantiate this, as complete scrambling has occurred in AE133 prior to the selective cleavage at Asp. Sequestering of protons by basic residues does therefore not inhibit the proton traffic that causes scrambling to any measurable extent.

Conclusion

We have utilized a unique set of peptides having a receptor binding and a nonbinding region thus enabling a polarized, regioselective deuterium incorporation of the peptide depending on its receptor binding status during the exposure to deuterated solvent. Upon conventional CID in a quadrupole-time-of-flight (Q-TOF) mass spectrometer, complete scrambling among all N and O-linked hydrogens was observed for both b- and y-fragment ions. These receptor-binding peptides represent ideal target peptides for future studies exploring other fragmentation mechanisms/conditions for maintenance of the original deuteration pattern present in the intact peptide. It would for instance be interesting to investigate whether fragmentation under high-energy collisional activation or electron capture dissociation is better suited for preservation of the receptor induced deuterium “foot-print” on the peptide.

Acknowledgment. This work was supported by grants from the Danish Instrument Biotechnology Center (DABIC), The Lundbeck Foundation, the Carlsberg Foundation, the John and Birthe Meyer Foundation. The authors thank Dr. Shabaz Mohammed (University of Southern Denmark) for helpful discussions and critical comments on the manuscript.

JA043789C

- (47) Hagman, C.; Hakansson, P.; Buijs, J.; Hakansson, K. *J. Am. Soc. Mass Spectrom.* **2004**, *15*, 639–646.
- (48) Wysocki, V. H.; Tsaprailis, G.; Smith, L. L.; Brecht, L. A. *J. Mass Spectrom.* **2000**, *35*, 1399–1406.
- (49) Yalcin, T.; Khouw, C.; Csizmadia, I. G.; Peterson, M. R.; Harrison, A. G. *J. Am. Soc. Mass Spectrom.* **1995**, *6*, 1165–1174.
- (50) Yalcin, T.; Csizmadia, I. G.; Peterson, M. R.; Harrison, A. G. *J. Am. Soc. Mass Spectrom.* **1996**, *7*, 233–242.
- (51) Klassen, J. S.; Kebarle, P. *J. Am. Chem. Soc.* **1997**, *119*, 6552–6563.
- (52) Cordero, M. M.; Houser, J. J.; Wesdemiotis, C. *Anal. Chem.* **1993**, *65*, 1594–1601.
- (53) Cordero, M. M.; Wesdemiotis, C. *Org. Mass Spectrom.* **1994**, *29*, 382–390.
- (54) Csonka, I. P.; Paizs, B.; Lendvay, G.; Suhai, S. *Rapid Commun. Mass Spectrom.* **2000**, *14*, 417–431.
- (55) Csonka, I. P.; Paizs, B.; Lendvay, G.; Suhai, S. *Rapid Commun. Mass Spectrom.* **2001**, *15*, 1457–1472.
- (56) Paizs, B.; Csonka, I. P.; Lendvay, G.; Suhai, S. *Rapid Commun. Mass Spectrom.* **2001**, *15*, 637–650.
- (57) Rodriguez, C. F.; Cunje, A.; Shoeib, T.; Chu, I. K.; Hopkinson, A. C.; Siu, K. W. M. *J. Am. Chem. Soc.* **2001**, *123*, 3006–3012.